IEEE Open Journal of
Circuits and Systems

Received 7 January 2023; revised 10 February 2023; accepted 18 February 2023. Date of publication 22 February 2023; date of current version 22 March 2023.

Digital Object Identifier 10.1109/OJCAS.2023.3247573

Adaptive Control Technique for Portable Solar Powered EV Charging Adapter to Operate in Remote Location

NISHANT KUMAR[1] (Senior Member, IEEE), HARSHIT KUMAR SINGH[2], AND ROLAND NIWAREEBA[3] (Member, IEEE)

[1]Department of Electrical Engineering, Indian Institute of Technology Jodhpur, Jodhpur 342030, India

[2]Department of Electrical Engineering, Indian Institute of Technology Delhi, New Delhi 110016, India

[3]Department of Electrical and Electronic Engineering, Kyambogo University, Kampala, Uganda

This article was recommended by Guest Editor F. Bizzarri.

CORRESPONDING AUTHOR: R. NIWAREEBA (e-mail: rniwareebakyu@gmail.com).

ABSTRACT Every EV (Electric Vehicle) comes with limited energy storing capability. After travelling a certain distance, a charging facility is required to recharge the EV batteries, which is easy to be made available in cities. But, in remote locations, charging service is challenging. Therefore, big countries like USA, Canada, China, Russia, India, Australia, and few Arabian countries are planning to provide pillar top solar panels on remote locations for EV charging in emergency situations. To operate in this situation, a special charging adapter is required to extract maximum power from the panel using the MPPT (Maximum Power Point Tracking) technique, monitor the charging current, and safely complete the charging process. In this paper, a single sensor-based economical charging adapter is presented for EVs to fulfil this objective. Moreover, the Single Input Fuzzy Logic tuned Deterministic Optimization (SIFL-DO) algorithm is proposed to accomplish MPPT operation and battery charging management. Because of its low cost and fast response, the single current sensor-based charging adapter is highly economical. Additionally, the SIFL-DO algorithm has very good condition estimation and decision-making capability, which accurately performs MPPT and charging management. In this work, the capability of the developed adapter with the SIFL-DO algorithm is evaluated on Hardware prototype. Also, comparative studies are performed w.r.t. state-of-the-art techniques. Further to determine the industry's suitability, the developed technique is tested on European Standard EN50530.

INDEX TERMS Solar PV, EV, battery charging, MPPT, sensor-less scheme.

I. INTRODUCTION

ELECTRIC Vehicles (EVs) have shown to be a viable alternative to hydrocarbon automobiles considering they emit no greenhouse gas and do not rely on crude oil-producing countries to determine gas prices. Other than this the entire full energy cycle is more efficient in the case of renewable energy, notably for solar photovoltaic (SPV) energy generation. We can readily observe how electricity rates remain reasonably stable while fuel costs surge throughout every international conflict. Considering all of these factors, electric vehicles are a better substitute to gasoline-powered vehicles. Whereas a significant amount of work is being undertaken to develop efficient electric vehicles and their corresponding infrastructural facilities, electric vehicles primarily use two charging schemes: on-board charging and off-board charging. The charging circuit of the on-board is retained within the automobile itself, and it may be charged whether using AC or DC. The charging circuit is housed within the charging station in the case of the off board, and an EV may indeed be charged using either 1-phase AC, 3-phase AC, or DC power, each of which has advantages as well as disadvantages. Charging an EV using solar energy can be a difficult operation considering solar irradiance and temperature change over time, contrary to an

idealistic situation where weather conditions and temperature are constant [1]. As a result, the power generated is indeed not uniform. Various conventional mathematical and neural computing-based optimization approaches and techniques are implemented to assess this and it is known as "Maximum power point tracking (MPPT) of solar arrays [2], and each MPPT algorithm setup has advantages as well as disadvantages. This is implemented in series with the circuit referred to as the DC-DC Buck/Boost converter, whereby the solar panel's power output may very well be regulated by numerous MPP control methods mentioned above by altering the converter's pulse width modulated (PWM) input signal. Using this, solar panels are maintained at their maximum power point (Vmp, Imp), going to charge the EV at the solar PV's maximum power output [3]. Further to that, since solar photovoltaic systems can be broadly classified as grid-connected or remote stand-alone systems, the system's power capacity can differ widely from low-powered operation to high-powered operation, the median generation capacity can differ of these systems is still well above hundreds of kW (kilo-Watts). It is also known that a sizable SPV can produce hundreds of amps of direct current, which also, if connected directly into the Electric vehicle, can cause damage [4].

In literature, different solutions for PV-powered EV chargers are proposed, such as Multifunctional Off-Board EV Charger [5], Bidirectional EV Charger [6], Z-Source based charger [7], Wireless EV Charger [8], Intermittency mitigated EV Charger [9], etc. All these chargers are absolutely fine and suitable for EVs. However, in all these configurations and topologies, the grid is mandatory with PV to operate during the charging process. In the case of the standalone condition, these techniques will not work. Therefore, this paper proposes a novel topology and control to operate in a standalone condition.

Additionally, an EV has a charging current rating that ordinarily ranges from 10% to 15% of the maximum capacity of the EV battery, with most EVs receiving up to 32A for power delivery up to 7.4KWs from a typical charger, where the EV's battery is not continuously cooled throughout this charging period. Consequently, current must be monitored before being supplied into the EV [10], which may be performed by analyzing the solar array's output with sensors [11], [12]. Therefore, although solar PV can be found in even the most sparsely populated areas due to the increased intervention from the government, EV chargers are currently difficult to discover even those in tier 2 or 3 cities, let alone in villages or isolated areas. And hardly any research has been dedicated to the accessibility of charging infrastructure in remote locations where, if an EV user becomes stuck, they would have been unable to use an EV charging station since incorporating complex and costly charging stations for electric may not even be very economical in areas where the number of consumers is rather relatively small, as well as remote locations make it much more difficult for repair or replacement, which arises as a potential hazard which will always be considered as part.

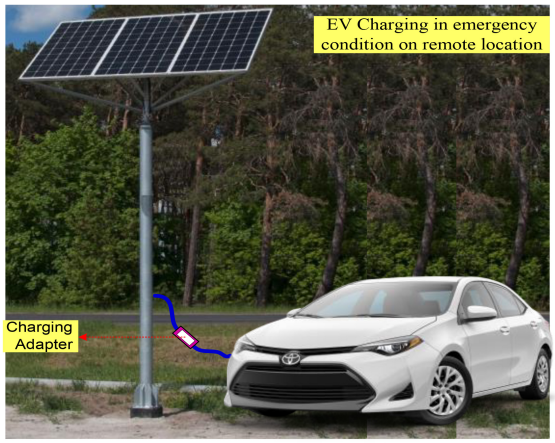

FIGURE 1. EV charging infrastructure on remote location.

These characteristics summarize the fact that this is not the real solution to this particular circumstance. Therefore, in big countries like the USA, Canada, China, Russia, India, Australia, as well as in a few Arabian countries, governments are planning to provide pillar top solar panels in the remote locations for EV charging in an emergency situation (such as shown in Fig. 1). To operate in this situation, a special charging adapter requires, which extracts maximum power from the panel using MPPT technique and monitors charging current and safely completes the charging process.

Therefore, as conclusion, can see the need for a compact, cost-effective charging solution that can be immediately linked to any Photovoltaic system and stored within the car and utilized in cases, for example like these as well as routine everyday charging needs and requirements. Even if certain work is underway in this area as well, wherein multiple sensors are being used to control the power fed into the Electric vehicle based on the capacity of the battery [13], [14], it uses a large number of sensor nodes, making it bulky and expensive, as well as increasing the possibility of electro-magnetic interference in the system. Furthermore, there is unquestionably no system on the market that can accomplish these two objectives, namely effective MPPT operating of solar photovoltaic and current strictly controlled charging of EV.

In this paper, both maximum power point tracking of solar photovoltaic array and controlling the current fed into the electric vehicle to charge the EV Battery safely as per the current limit, Single Input Fuzzy Logic tuned Deterministic Optimization (SIFL-DO) method is proposed. Moreover, for both the operation single sensor is been used to monitor and control the output of the solar PV array and current that is fed into the EV for charging its. Further to through experimental results the proposed method shows the clear advantage it offers in its operation as the step change is not a fixed constant but a variable in nature. Comparison is made with different leading state-of-the-art algorithms, which certainly demonstrates the leading edge of our proposed SIFL-DO methodology. Moreover, efficiency was tested to see the

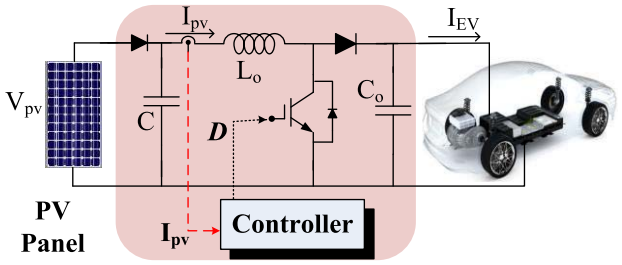

FIGURE 2. Single sensor-based circuit of EV charging adapter.

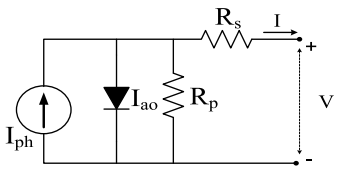

FIGURE 3. Solar PV cell electrical model.

industry redness of the method based upon the European standard (ES), i.e., EN50530 [15].

II. SYSTEM LAYOUT

The proposed model of the complete charging setup is shown in Fig. 1, where as per the circumstance when EV needs to be charged in any remote location can be directly linked to any available solar panels in that location using our proposed method, which in this case is shown as a complete solution as charging adapter, Fig. 2 represents the circuitry involved in it. Moreover, the EV can be connected along with the adapter to any solar PV even if the solar has no circuitry attached to it. The charging adapter will contain the circuitry for both the MPPT scheme and the charging current control scheme.

A. COMPLETE MODEL SETUP

In Fig. 2, the proposed charging adapter model is given, which shows a solar power monitoring sensor (current sensor), DC-DC Boost converter, and proposed SIFL-DO controller. Moreover, the whole circuitry will be kept inside the vehicle for on-board charging or in a box for off-board charging.

B. SOLAR PV CELL

Fig. 3 is the Electrical model of a solar PV cell which Eqn. (1) describes the Single Diode Solar PV model as shown in Fig. 3. Where I_{Ph} and I_S are the PV current and Reverse Saturation current of the solar cell further V_T being the Thermal voltage while V is the output voltage of the module of the solar PV cells connected in series, R_s is the equivalent series and parallel resistance of the cell V_T= k*T*a/q with 'n' series-connected cells while 'k' is the Boltzmann constant (1.3806503×10^(−23) J/K), "T" is the p-n junction temperature and "a" is ideality constant of Diode. 'q' is the charge (of an electron) [1.60217646×10-19 C].

$$I = I_{Ph} - I_S\left[exp\left(\frac{V + IR_S}{nV_T}\right) - 1\right] \tag{1}$$

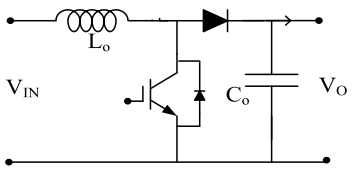

FIGURE 4. DC-DC boost converter.

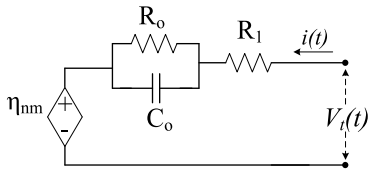

FIGURE 5. Electrical equivalent circuit of lithium-ion battery.

C. DC-DC BOOST CONVERTER

In below shown Fig. 4 DC-DC Boost Converter is presented, which is to be connected between the Solar PV Array and EV as shown in Fig. 2.

The voltage equation of the Ideal converter is given by;

$$V_O = \frac{V_{IN}}{(1 - D)} \tag{2}$$

In the practical converter, after taking losses of MOSFET and Diode into account. Output voltage is derived as;

$$V_O = \left(\frac{V_{IN} - V_{SW}D}{(1 - D)}\right) - V_D \tag{3}$$

For EV, it can be derived as;

$$V_{CHARGING} = \frac{V_{PV}}{(1 - D)} \tag{4}$$

$$V_{CHARGING} = \left(\frac{V_{PV} - V_{SW}D}{(1 - D)}\right) - V_D \tag{5}$$

where D is the Duty Cycle.

III. CONTROL SCHEME

In a single sensor-based EV charging adapter (SS-EVCA), the first objective is maximum power extraction from solar PV array. The second objective is charging current monitoring and keeping in a safe region. In the SS-EVCA scheme, the maximum solar panel power is regulated by maximizing the load transfer power.

In Fig. 5, η_{nm} is open circuit cell voltage, R_1 represents electrolyte resistance. R_O represents the charge transfer resistance, that models the voltage drop over the electrode-electrolyte interface due to a load. C_O represents double-layer capacitance, that models the effect of charges building up in the electrolyte at the electrode surface. Battery current and voltage are denoted as $i(t)$ and $V_t(t)$. Here, during charging, the voltage relationship is as follows.

$$\eta_{nm} < V_t(t) \tag{6}$$

The current equations are derived as,

$$\eta_{nm} = V_t(t) - i(t)R_1 - v_{Ro}(t) \tag{7}$$

$$\eta_{nm} = V_t(t) - i(t)R_1 - i_{Ro}(t)R_0 \tag{8}$$

The $i_{RCo}(t)$ is derived as,

$$\left.\begin{aligned} i_{Co}(t) = C_O \dot{v}_{Co}(t) &= C_O[\dot{i}_{Ro}(t) R_0] \\ i_{Ro}(t) + R_0 C_O \tfrac{di_{Ro}(t)}{dt} &= i(t) \end{aligned}\right\} \quad (9)$$

$$\frac{di_{Ro}(t)}{dt} = \frac{1}{R_0 C_O}\left(i(t) - i_{Ro}(t)\right) \quad (10)$$

$$\left.\begin{aligned} -R_0 C_O \tfrac{di_{Ro}(t)}{dt} &= i_{Ro}(t) - i(t) \\ \ln|i_{Ro}(t) - i(t)| &= \tfrac{-1(t+\lambda)}{R_0 C_O} \end{aligned}\right\} \quad (11)$$

$$i_{Ro}(t) = e^{\frac{-1(t+\lambda)}{R_0 C_O}} + i(t) \quad (12)$$

By using (12) and (8), the $V_t(t)$ is derived as,

$$V_t(t) = \eta_{nm} + i(t)R_1 + \left(e^{\frac{-1(t+\lambda)}{R_0 C_O}} + i(t)\right)R_0 \quad (13)$$

The charging power is derived as,

$$P_{Charge}(t) = V_t(\mathrm{t}) \times i(t) \quad (14)$$

$$P_{Charge}(t) = \left(\eta_{nm} + \ i(t)R_1 + \left(e^{\frac{-1(t+\lambda)}{R_0 C_O}} + i(t)\right)R_0\right) \times \ i(t) \quad (15)$$

In SS-EVCA, a DC-DC boost converter has been used, so $i(t)$ is derived as,

$$i(t) = (1 - D) \times I_{PV} \quad (16)$$

In EV, the load is a lithium-ion battery, so the charging power of the lithium-ion battery is derived as follows. Where, D is the duty cycle of the DC-DC converter. λ is an initial time constant of the capacitor. I_{pv} and V_{pv} are PV current and voltage, respectively From (19), it is clear that the EV charging power is the function of I_{PV} and D. Therefore, the sensed I_{PV} and calculated D values are enough to complete the task in the maximum power extraction process. Here to calculate the optimal values of D, a Deterministic Optimization" (DO) algorithm has been used, where for adaptive behavior a correction factor ω has been used. To generate the value of ω, a single input fuzzy logic (SIFL) controller is used.

Finally charging power is derived as,

$$P_{Charge}(t) = \left(\begin{array}{c} \eta_{nm} + ((1-D) \times I_{PV})R_1 + \\ \left(e^{\frac{-1(t+\lambda)}{R_0 C_O}} + ((1-D) \times I_{PV})\right)R_0 \end{array}\right) \times \left(\begin{array}{c} (1-D) \\ \times I_{PV} \end{array}\right) \quad (17)$$

$$P_{Charge}(t) = \max f(I_{PV}) \quad (18)$$

The objective function is derived as,

$$\max\left(P_{Charge}(t)\right) = \max\left[\left(\left(\begin{array}{c} \eta_{nm} + ((1-D) \times I_{PV})R_1 + \\ \left(e^{\frac{-1(t+\lambda)}{R_0 C_O}} + \left(\begin{array}{c} (1-D) \\ \times I_{PV} \end{array}\right)\right)R_0 \end{array}\right) \times \left(\begin{array}{c} (1-D) \\ \times I_{PV} \end{array}\right)\right] \quad (19)$$

The working objective of SIFL controller is to generate the values of ω according to the change in I_{PV}. The equation

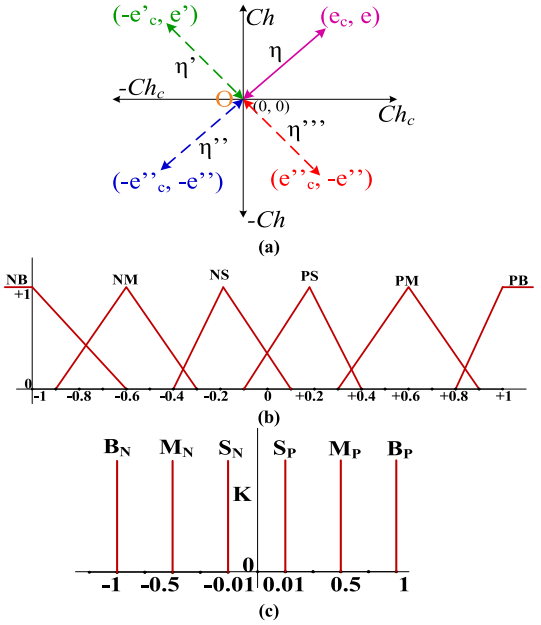

FIGURE 6. SFIL, (a) Representation of η, (b) Input membership functions, (c) output membership functions and control surface.

TABLE 1. Fuzzy logic rule table.

Input Rules						
	LDV_{-2}	LDV_{-1}	LDV_{-0}	LDV_{+0}	LDV_{+1}	LDV_{+2}
η	NB	NM	NS	PS	PM	PB
Output Rules						
	LDV_{-2}	LDV_{-1}	LDV_{-0}	LDV_{+0}	LDV_{+1}	LDV_{+2}
K	B_N	M_N	S_N	S_P	M_P	B_P

of change pattern (Ch) is derived as,

$$Ch = I_{PV}(t) - I_{PV}(t-1) \quad (20)$$

As inputs, errors and changes in errors are used in the conventional fuzzy controller. Because of these two inputs, the fuzzy rule table takes a large space on two dimensions plane. However, in the proposed SIFL, the rule table takes small space on one dimension plane. Here, as an input, the diagonal distance of rate of change (Ch_c) and change (Ch) coordinate from the origin is used. The diagonal distance (η) calculation and pictorial representation is shown in Fig. 6(a). The minimization of η is the key objective of SIFL. The η is derived as,

$$\eta = \sqrt{Ch^2 + Ch_c^2} \quad (21)$$

To fulfil the objective of SIFL, it follows a particular set of rules for the input member function and output member function, and according to the control surface, SIFL decides an optimal action. The input and output membership functions with control surface are shown in Fig. 6(b) & Fig. 6(c), respectively. Moreover, the input and output rule tables for SIFL are given in Table 1. Where, LDV is the linguistic value of η. NB, NM, NS, PS, PM, and PB are negative

big, negative medium, negative small, positive small, positive medium and positive big value of η. B_N, M_N, S_N, B_P, M_P and S_P are big negative, medium negative, small negative, big positive, medium positive, and small positive output value of ω. The optimal value of ω, drive the solar PV panel according to the decided mode of operation.

Here, $P_{Charge}(t)$ is the function of D. Therefore, the calculation of D is very important. The operating behavior of the system depends on D and I_{PV}. By using these two parameters, I_{ref} is calculated, which is derived as,

$$I_{ref}(t) = (1 - D) \times I_{PV}(t) \tag{22}$$

When calculated I_{ref} is greater than EV battery nominal charging current rating (I_{Bnom}), then solar PV panel will operate under protection mode. It means the available solar PV panel power is more than the required power during charging. Moreover, when calculated I_{ref} is less than the EV battery nominal charging current rating (I_{Bnom}), then solar PV panel will operate under MPPT (Maximum Power Point Tracking) mode. It means that available solar PV panel power is less than or equal to the required power during charging.

$$\left.\begin{array}{r} I_{ref} > I_{Bnom} \Rightarrow protection \text{ mode} \\ protection \text{ mode} \Rightarrow P_{PVav} > P_{EVr} \end{array}\right\} \tag{23}$$

$$\left.\begin{array}{r} I_{ref} \leq I_{Bnom} \Rightarrow MPPT \text{ mode} \\ MPPT \text{ mode} \Rightarrow P_{PVav} \leq P_{EVr} \end{array}\right\} \tag{24}$$

where, P_{PVav} is available PV power, P_{EVr} is the power safety rating of EV.

Here, based upon the value of I_{ref}, EV Modes are selected, which are as MPPT mode or protection mode, as shown in (23) and (24). Current is continuously monitored and therefore, accordingly I_{ref} is changed to get the desired operating current.

A. PROTECTION MODE

This condition arises when Eqn. (23) will be satisfied. It is basically, the current I_{ref} is higher than the rated EV charging current. Therefore, in protection mode current is brought down to the rated current. In this situation, by using "Deterministic Optimization" (DO) algorithm, the optimal $D(t)$ is generated using ω. In DO algorithm, $P_{Charge}(t)$, and $I_{PV}(t)$ are used for decision making, and finally, $D(t+1)$ is regulated accordingly.

$$\left.\begin{array}{r} If : \Delta P_{Charge}(t) > 0 \& \Delta I_{PV}(t) > 0 \rightarrow Decrement \text{ in } D \\ If\ else : \Delta P_{Charge}(t) > 0 \& \Delta I_{PV}(t) < 0 \rightarrow Increment \text{ in } D \\ If\ else : \Delta P_{Charge}(t) < 0 \& \Delta I_{PV}(t) > 0 \rightarrow Increment \text{ in } D \\ If\ else : \Delta P_{Charge}(t) < 0 \& \Delta I_{PV}(t) < 0 \rightarrow Decrement \text{ in } D \end{array}\right\} \tag{25}$$

Equation (25) can be written as;

$$\left.\begin{array}{r} If : (\Delta P_{Charge}(t) > 0 \& \Delta I_{PV}(t) > 0) || (\Delta P_{Charge}(t) < 0 \& \Delta I_{PV}(t) < 0) \Rightarrow D \downarrow \\ else : (\Delta P_{Charge}(t) > 0 \& \Delta I_{PV}(t) < 0) || (\Delta P_{Charge}(t) < 0 \& \Delta I_{PV}(t) > 0) \Rightarrow D \uparrow \end{array}\right\} \tag{26}$$

The pseudo-code DO for protection mode of operation is given as follows,

begin (DO)
$\Delta P_{Charge}(t) = P_{Charge}(t) - P_{Charge}(t-1)$
$\Delta I_{PV}(t) = I_{PV}(t) - I_{PV}(t-1)$
if $(\Delta P_{Charge}(t) > 0)$
  if $(\Delta I_{PV}(t) > 0) \Rightarrow D(t+1) = D(t) - \omega$
  else $\Rightarrow D(t+1) = D(t) + \omega$ *end*;
else { if $(\Delta I_{PV}(t) > 0) \Rightarrow D(t+1) = D(t) + \omega$; else $\Rightarrow D(t+1) = D(t) - \omega$; *end* }
end

B. MPPT OPERATION

This condition arises when Eqn. (24) will be satisfied. It is basically, the current I_{ref} is lower than the rated EV charging current. Therefore, in protection mode current is brought up to the MPP current. In this situation, by using DO algorithm, the optimal D is generated. DO algorithm related equations and condition for D generation is as follows.

$$\left.\begin{array}{r} If : \Delta P_{Charge}(t) > 0 \& \Delta I_{PV}(t) > 0 \rightarrow Increment \text{ in } D \\ If\ else : \Delta P_{Charge}(t) > 0 \& \Delta I_{PV}(t) < 0 \rightarrow Decrement \text{ in } D \\ If\ else : \Delta P_{Charge}(t) < 0 \& \Delta I_{PV}(t) > 0 \rightarrow Decrement \text{ in } D \\ If\ else : \Delta P_{Charge}(t) < 0 \& \Delta I_{PV}(t) < 0 \rightarrow Increment \text{ in } D \end{array}\right\} \tag{27}$$

Equation (27) can be written as;

$$\left.\begin{array}{r} If : (\Delta P_{Charge}(t) > 0 \& \Delta I_{PV}(t) > 0) || (\Delta P_{Charge}(t) < 0 \& \Delta I_{PV}(t) < 0) \Rightarrow D \uparrow \\ else : (\Delta P_{Charge}(t) > 0 \& \Delta I_{PV}(t) < 0) || (\Delta P_{Charge}(t) < 0 \& \Delta I_{PV}(t) > 0) \Rightarrow D \downarrow \end{array}\right\} \tag{28}$$

The pseudo-code DO for MPPT mode of operation is given as follows,

begin (DO)
$\Delta P_{Charge}(t) = P_{Charge}(t) - P_{Charge}(t-1)$
$\Delta I_{PV}(t) = I_{PV}(t) - I_{PV}(t-1)$
if $(\Delta P_{Charge}(t) > 0)$
  if $(\Delta I_{PV}(t) > 0) \Rightarrow D(t+1) = D(t) + \omega$
  else $\Rightarrow D(t+1) = D(t) - \omega$; *end*
else $\Rightarrow$ { if $(\Delta I_{PV}(t) > 0) \Rightarrow D(t+1) = D(t) - \omega$; else $\Rightarrow D(t+1) = D(t) + \omega$; *end* }
end

In SS-EVCA controller, using the information of $I_{PV}(t)$, the optimal value of $D(t+1)$ is calculated. The SS-EVCA controller diagram is shown in Fig. 7.

IV. RESULTS AND DISCUSSIONS

For the purpose of testing the proposed approach, a hardware prototype is created, which is shown in Fig. 8. The equipment used for it is Auxiliary power supply (HTC Instruments DC 3005 DC 5A Linear Power Supply), two PLECS - RT Platform (RT Box 1 - Plexim, Processor.

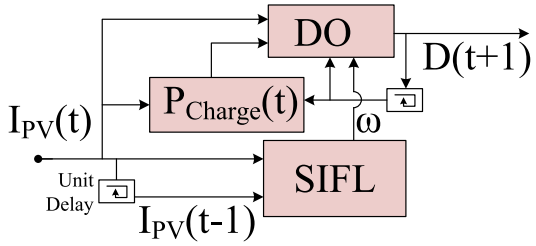

FIGURE 7. SS-EVCA controller.

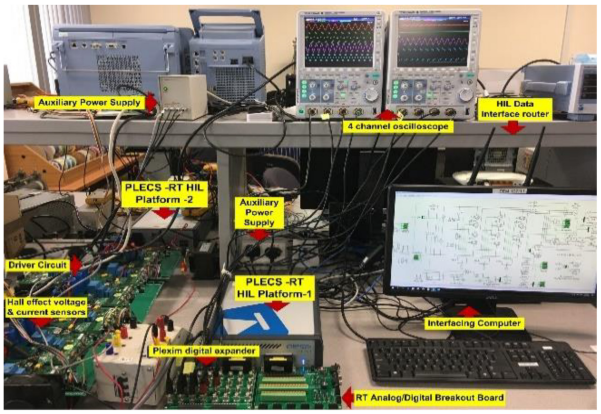

FIGURE 8. Photograph of the experimentation setup.

Xilinx Zynq Z-7030.), four channel oscilloscope (Tektronix 110 GHz), Driver Circuit, Hall effect voltage sensor (LV-25) and current sensor (LA-55p), Plexim digital expander, Interfacing computer, Data interface router and RT Analog/ Digital Breakout Board. Moreover, the circuit parameters are as follows. Inductor of DC-DC Converter (Lo)= 100 mH, PV link Capacitor(C)=3.12μF, Switching frequency = 10kHz, Capacitor of DC-DC Converter (Co)=1000μF, Solar panel short circuit current (Isc)=31.5A, Solar panel open circuit voltage (Voc)=182V, and Battery Nominal Voltage=250V. Hardware experiments were carried out on three algorithms in particular: Perturb & Observe (P&O) [12], Modified Perturb & Observe (MP&O) [11], and proposed SIFL-DO. Further tests are carried out on these three algorithms.

Furthermore, the solar irradiance range was varied widely and classified into two main categories, Case 1 and Case 2, with comparisons made in both cases on the basis of the characteristics curve developed during the experiments primarily for various Output parameters of the Solar PV array and thus based on the control algorithm and EV Battery charging characteristics of power that was fed into the EV.

A. CASE-1: SOLAR IRRADIANCE VARIATION IN STEP MANNER

In case-1, solar irradiance has been varied in a stepwise manner as shown in Fig. 9 for a period of 5 secs, i.e., from 0.5 secs to 5.5 secs and varies from initially 1000W/m^2 to 500W/m^2 to 900W/m^2 to 600W/m^2 to 800W/m^2 and finally

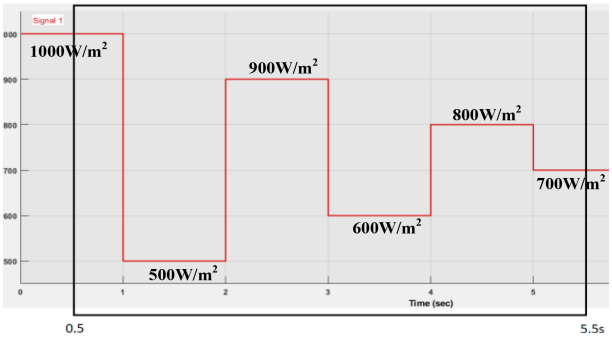

FIGURE 9. Solar irradiance pattern with step change.

to 700W/m^2 while the change in solar irradiance is in the stepped manner.

Here, output waveforms of solar PV are shown in Fig. 10, where Fig. 10(a) is for P&O [12], followed by Fig. 10(b) is for MP&O [11] and Fig. 10(c) is for our proposed approach SIFL-DO. In Fig. 10(a) and Fig. 10(b), it can be clearly seen that in the steady-state condition, the significantly high number of fluctuations are in PV voltage (V_{PV}), PV current (I_{PV}) and PV power (P_{PV}). This is happening because of the oscillating duty cycle generated by P&O and MP&O. The waveforms of the duty cycle obtained by P&O and MP&O algorithm are also shown in Fig. 10(a) and Fig. 10(b), respectively.

Moreover, during dynamic change conditions, time taken to transition from one mode of operation to another is clearly taking more time in the case of P&O [12] and MP&O [11] due to their rigid and constant nature of step size. While comparing Fig. 10(a), Fig. 10(b) that is P&O and MP&O, respectively, with Fig. 10(c) that is our proposed method SIFL-DO, these unwanted fluctuations are removed significantly in steady-state conditions, and in dynamic change conditions, transition time is much faster which can be clearly noticed between 0.5s to 2.5s. Moreover, in steady-state conditions this fluctuation becomes complete negligible.

The waveforms of EV battery charging are shown in Fig. 11, where Fig. 11(a), Fig. 11(b), and Fig. 11(c) depict the performance of P&O [12], MP&O [11] and proposed SIFL-DO algorithm. In Fig. 11(a) and Fig. 11(b), it can be clearly seen that in steady-state conditions, oscillations are in EV battery charging voltage (V_{EV}), EV battery charging current (I_{EV}) and EV battery charging power (P_{EV}). This is happening because of oscillations in V_{PV}, I_{PV}, and P_{PV}, because of P&O and MP&O. Moreover, during dynamic change conditions, the time taken to transition from one power level to another, it is taking longer time, which disturbs the charging process and reduces the efficiency of the system. However, Fig. 11(c) shows that because of our proposed method SIFL-DO, the oscillations in the steady-state condition is negligible, and in dynamic change condition, transition time is much faster, which enhances the charging process and efficiency of the system.

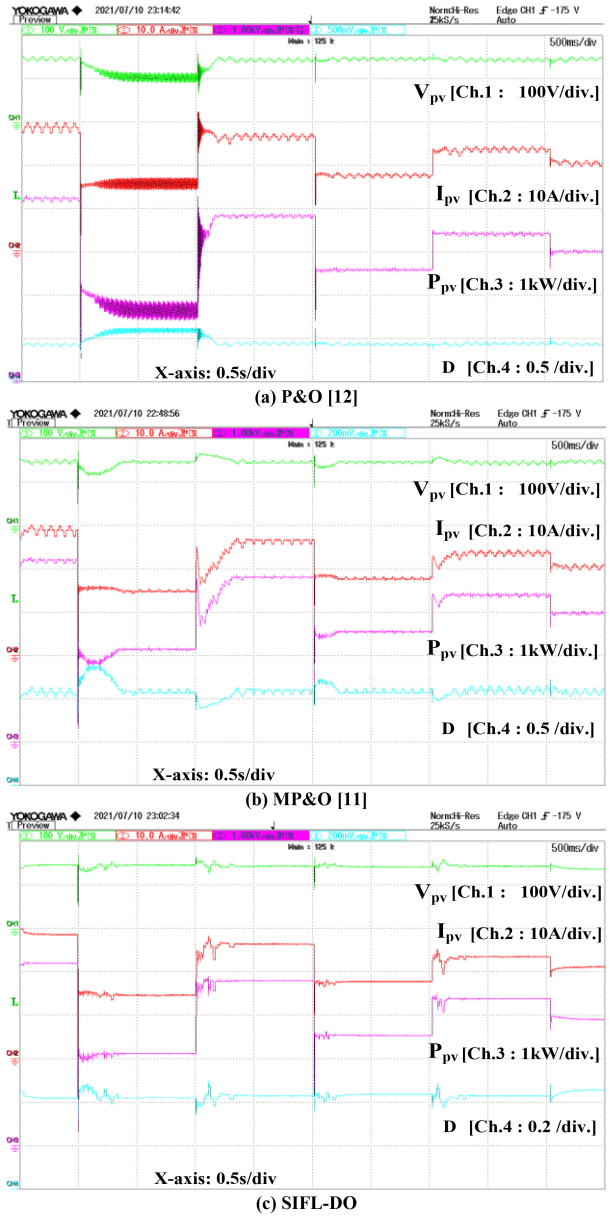

FIGURE 10. The obtained waveforms of solar panel in case-1 test condition by using (a) P&O [12], (b) MP&O [11] and (c) SIFL-DO algorithm.

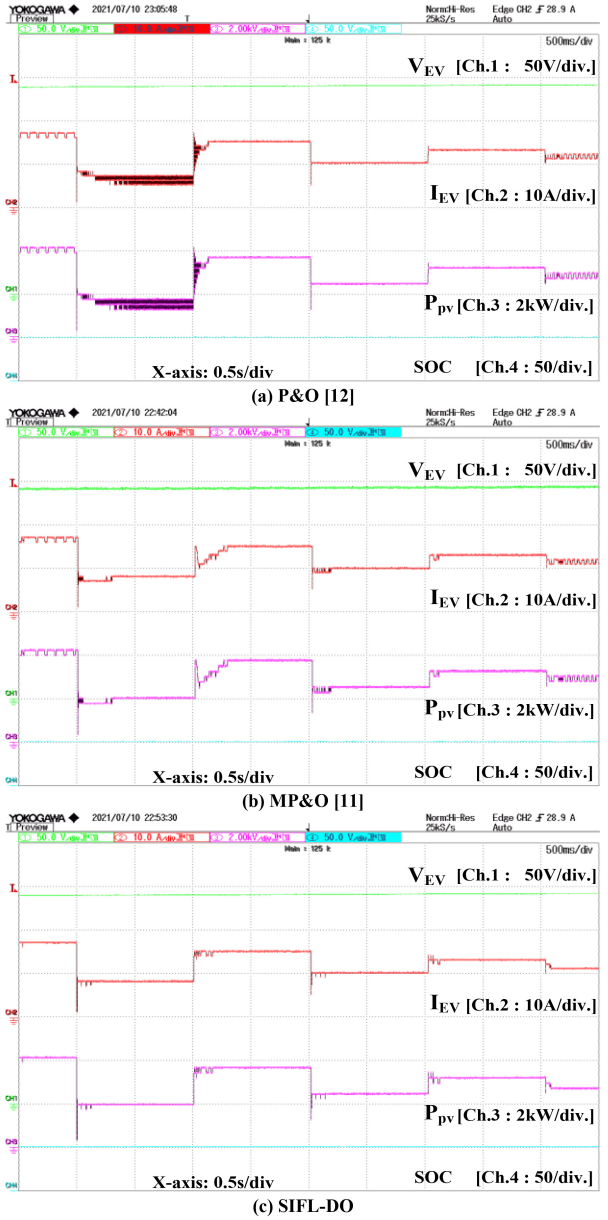

FIGURE 11. The obtained waveforms of EV charging process in case-1 test condition by using (a) P&O [12], (b) MP&O [11] and (c) SIFL-DO.

B. CASE-2: SOLAR IRRADIANCE VARIATION IN RAMP MANNER

In case-2, solar irradiance has been varied in ramp wise manner as shown in Fig. 12 for a time period of 5s, i.e., from 0.5s to 5.5s and varies from initially 1000W/m^2 to 400W/m^2 to 900W/m^2 to 500W/m^2 to 800W/m^2 and finally to 700W/m^2 while the change in solar irradiance is in a ramp manner.

In this condition, the obtained output waveforms of solar PV are shown in Fig. 13, where Fig. 13(a) is for P&O, followed by Fig. 13(b) is for MP&O and Fig. 13(c) is for our proposed approach SIFL-DO. In Fig. 13(a) and Fig. 13(b), it can be clearly seen that in steady-state condition, significantly huge fluctuations are in V_{PV}, I_{PV} and P_{PV}. This is happening because of the oscillating duty cycle generated by P&O and MP&O. The waveforms of D obtained by P&O and MP&O algorithm are also shown in Fig. 13(a) and Fig. 13(b), respectively. Moreover, during dynamic change condition, during shifting from one mode of operation to another, deviation on the tracking track is, in the case of P&O and MP&O, because of their rigid and constant nature of step size. While comparing Fig. 13(a), Fig. 13(b) that is P&O and MP&O, respectively with Fig. 13(c) that is our proposed method SIFL-DO, these unwanted fluctuations are removed significantly in steady-state conditions, and in dynamic change conditions, it is following the change with the slop of ramp. Moreover, during tracking, the fluctuation and deviations are completely negligible.

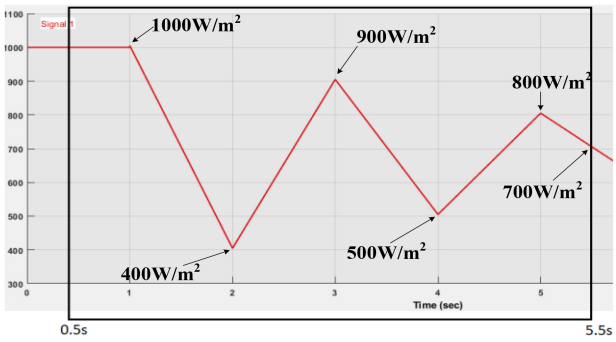

FIGURE 12. Solar irradiance pattern with ramp change.

The waveforms of EV battery charging are shown in Fig. 14, where Fig. 14(a), Fig. 14(b), and Fig. 14(c) depict the performance of P&O [12], MP&O [11] and proposed SIFL-DO algorithm. In Fig. 14(a) and Fig. 14(b), it can be clearly seen that in steady-state condition, oscillations are in V_{EV}, I_{EV} and P_{EV}. This is happening because of oscillations in V_{PV}, I_{PV}, and P_{PV}, because of P&O and MP&O. Moreover, during dynamic change condition, the deviation on the tracking track, during transition from one power level to another is clearly visible, which disturbs charging process and reduces the efficiency of the system. However, Fig. 14(c) shows that because of our proposed method SIFL-DO, the oscillations in the steady-state condition is negligible, and in the dynamic change condition, deviation on the tracking track is also negligible, which enhances the charging process and efficiency of the system.

C. CASE-3: EUROPEAN STANDARD EN50530

To conform the industrial suitability of the proposed SIFL-DO algorithm, it has been tested on European Standard (ES) EN50530. Testing is carried out, and efficiency is estimated for both steady-state and dynamic conditions.

1) STATIC EFFICIENCY

The static efficiency calculation procedure in ES En50530 is given in two ways: Firstly, the European efficiency (α_{Eu}) which is governed by (29) and secondly, the Californian efficiency (α_{Cl}), which is given by the (30) where % indicates about solar irradiance w.r.t. the base value (1000W/m^2), and α is the corresponding efficiency. The test results for both the cases are shown in Fig. 15 and Fig. 16, respectively.

The European efficiency (α_{Eu}) is expressed as,

$$\alpha_{Eu} = 0.03 \times \alpha_{5\%} + 0.06 \times \alpha_{10\%} + 0.13 \times \alpha_{20\%} + 0.10 \times \alpha_{30\%} + 0.48 \times \alpha_{50\%} + 0.20 \times \alpha_{100\%} \quad (29)$$

The Californian efficiency (α_{Cl}) is expressed as,

$$\alpha_{Cl} = 0.04 \times \alpha_{10\%} + 0.05 \times \alpha_{20\%} + 0.12 \times \alpha_{30\%} + 0.21 \times \alpha_{50\%} + 0.53 \times \alpha_{75\%} + 0.05 \times \alpha_{100\%} \quad (30)$$

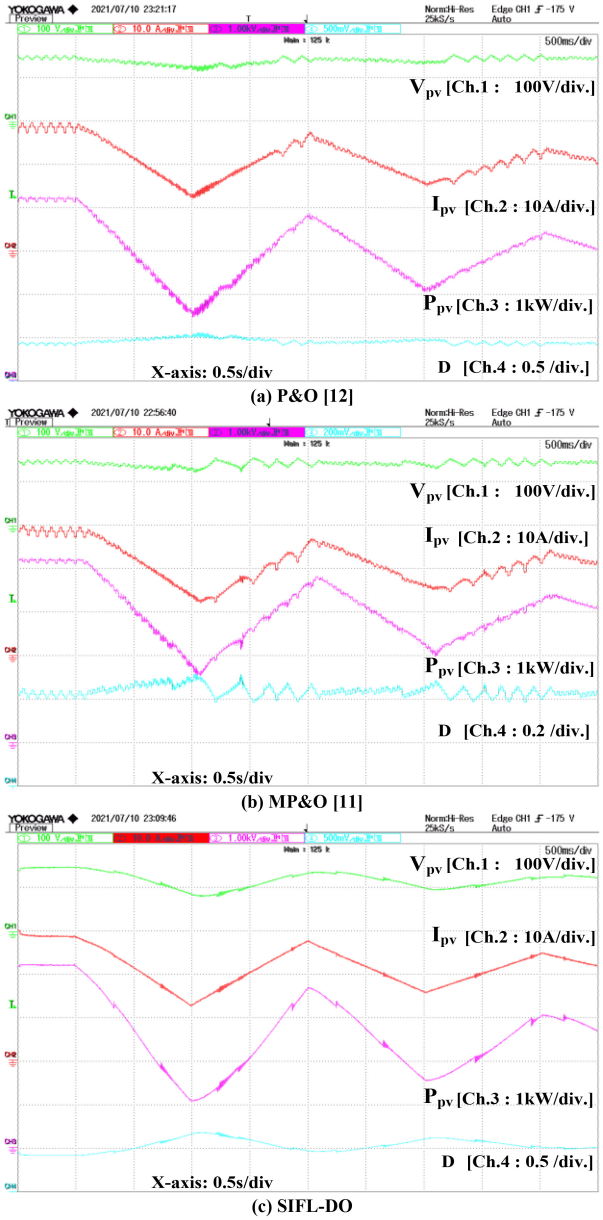

FIGURE 13. The obtained waveforms of solar panel in case-2 test condition by using (a) P&O, (b) MP&O and (c) SIFL-DO algorithm.

From (29) and Fig. 15, the $\alpha_{Eu} = 99.51\%$, and from (30) and Fig. 16, the $\alpha_{Cu} = 99.43\%$. Here, both of these observed efficiencies are greater than 99%. Therefore, according to the EN50530 standard, the proposed SIFL-DO is capable to perform on the industry level, which means in practical conditions.

2) DYNAMIC EFFICIENCY

In EN50530 standard, the test is performed in two types of irradiances change condition. Low to Medium irradiances change condition, where it varies in between 100 W/m^2 to 500 W/m^2, and another is Medium to High irradiances change condition, where it varies in between 300 W/m^2 to 1000 W/m^2. In both irradiance band, 2 types of irradiances

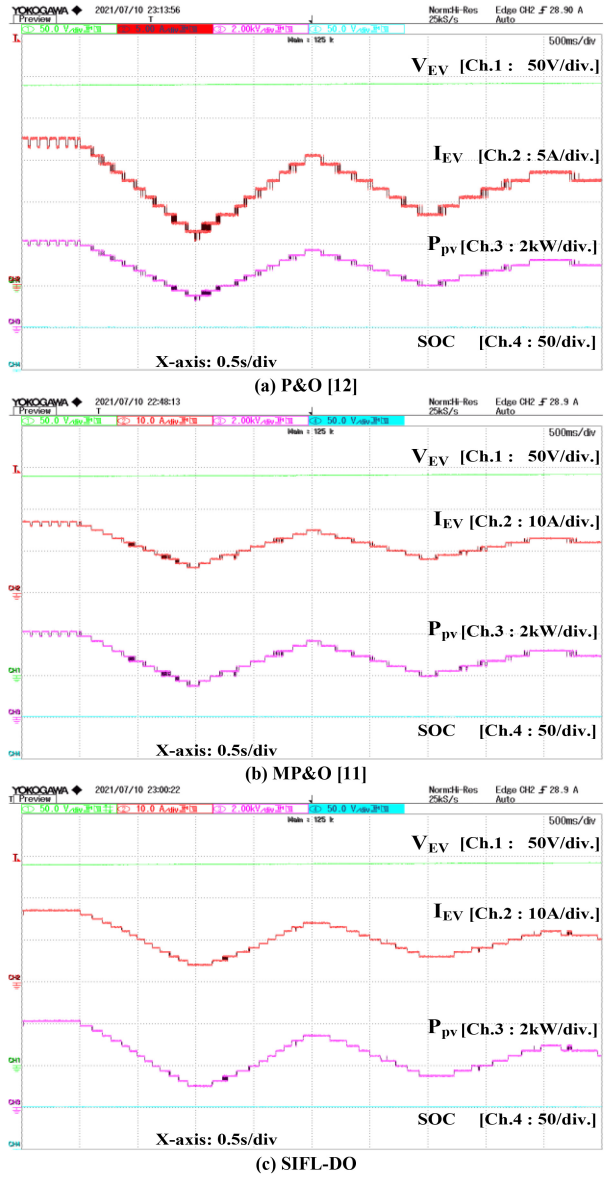

FIGURE 14. The obtained waveforms of EV charging process in case-2 test condition by using (a) P&O [12], (b) MP&O [11] and (c) SIFL-DO.

change slops are considered, which has given in Table 2, and efficiency calculation is given in Eqn. (31). Moreover, the obtained waveforms are shown in Fig. 17.

The equation of dynamic efficiency calculation is described as,

$$\alpha_{dy} = \frac{1}{€}\sum_{\hbar=1}^{€}\frac{\sum_{\hbar} Extracted\ P_{PV}}{\sum_{\hbar} Available\ P_{PV}} \tag{31}$$

Where € is a total number of sections of every insolation band.

From (31) and Fig. 17, the $\alpha_{dy} = 99.22\%$ during Low to Medium irradiances change conditions, and during Medium to High irradiances change conditions, the $\alpha_{dy} = 99.30\%$. The average $\alpha_{dy} = 99.26\%$. The results of all techniques are summarized in Table 3. Here, this obtained dynamic

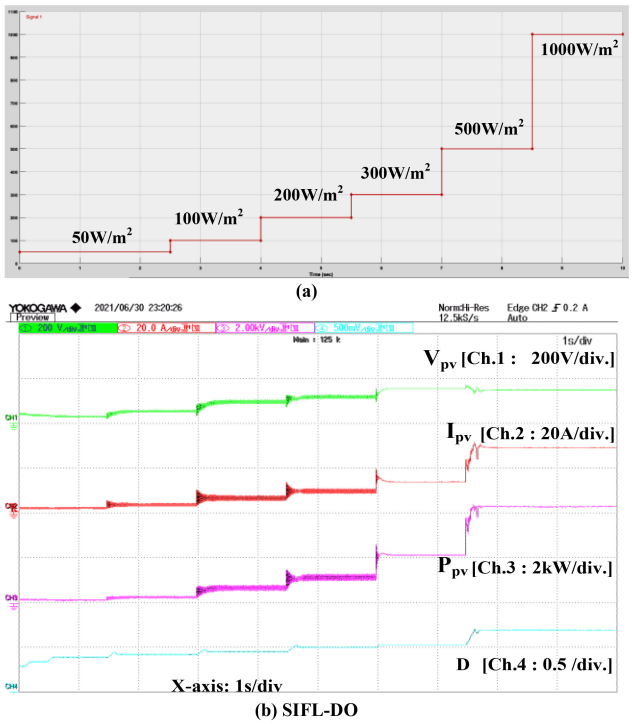

FIGURE 15. The obtained waveforms of SIFL-DO algorithm in European efficiency test condition.

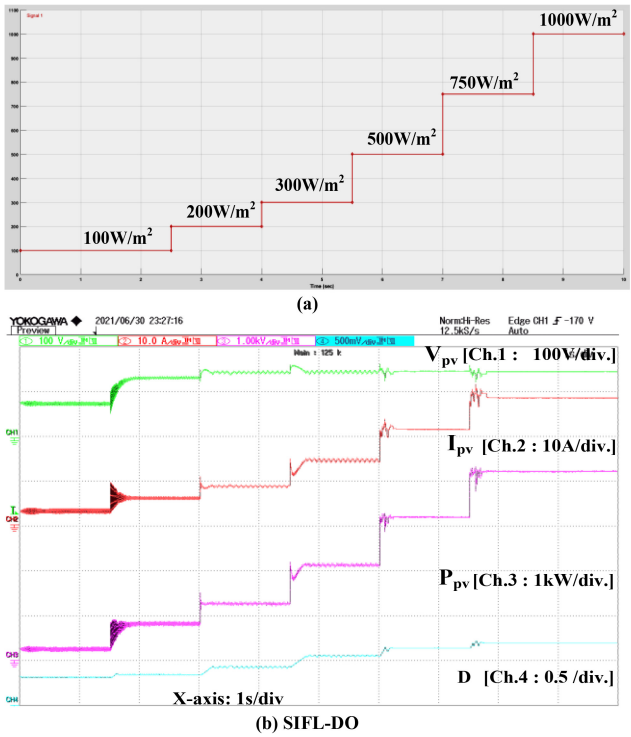

FIGURE 16. The obtained waveforms of SIFL-DO algorithm in Californian efficiency test condition.

efficiency is greater than 99%. Therefore, according to the EN50530 standard, the proposed SIFL-DO is suitable for industrial application.

TABLE 2. Dynamic test conditions.

Low to Medium - 100W/m^2 to 500W/m^2	
Serial No.	Ramp Slope
1	+50W/m^2/s to -50W/m^2/s
2	+100W/m^2/s to -100W/m^2/s
Medium to High - 300W/m^2 to 1000W/m^2	
Serial No.	Ramp Slope
1	+50W/m^2/s to -50W/m^2/s
2	+100W/m^2/s to -100W/m^2/s

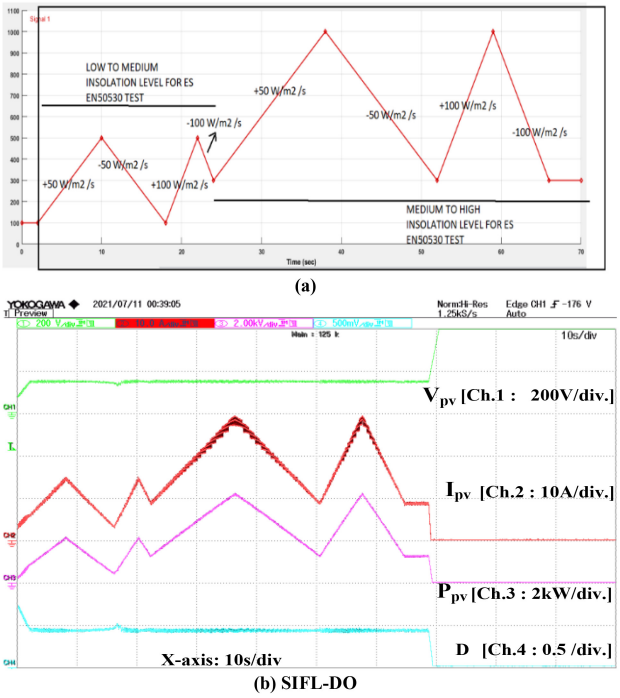

FIGURE 17. The obtained waveforms of SIFL-DO algorithm in dynamic efficiency test condition.

TABLE 3. EN50530 test results.

		P&O [12]	MP&O [11]	SIFL-DO
Static Efficiency	European Efficiency	97.56%	98.73%	99.51%
	Californian Efficiency	97.87%	98.22%	99.43%
Dynamic Efficiency		96.97%	98.31%	99.26%

V. CONCLUSION

In this paper, a novel charging adapter topology has been proposed, which is based on a single current sensor. Low cost, fast response and high sensitivity to dynamic change, these behaviors of the current sensor make it an accurate and economical charger. Moreover, a novel Single Input Fuzzy Logic tuned Deterministic Optimization (SIFL-DO) algorithm has been proposed to accomplish MPPT operation and battery charging management. SIFL-DO algorithm has very good condition estimation and decision-making capability, which performs MPPT very accurately, monitors the charging process, and keeps it safe in adverse conditions. The capability of developed charging adapter with SIFL-DO algorithm has been evaluated on Hardware prototype, as well as comparative studies have been performed w.r.t. state-of-the-art techniques, where developed charging scheme shows the dominancy over other techniques. The only limitation of this technique is required comparatively slightly bigger processer to execute this control logics. But, on industrial level, the use of this type of processer is very common. To prove the industrial suitability, the developed technology has been tested on European Standard (ES) EN50530, where it has been successfully satisfied the Standard charitarian. Therefore, the developed technology is an efficient and economical solution to EV charging in remote location using pillar top PV panels.

REFERENCES

[1] M. H. Mobarak, R. N. Kleiman, and J. Bauman, "Solar-charged electric vehicles: A comprehensive analysis of grid, driver, and environmental benefits," *IEEE Trans. Transport. Electrific.*, vol. 7, no. 2, pp. 579–603, Jun. 2021.

[2] C. S. Chiu, "T-S fuzzy maximum power point tracking control of solar power generation systems," *IEEE Trans. Energy Convers.*, vol. 25, no. 4, pp. 1123–1132, Dec. 2010.

[3] Y.-H. Liu, S.-C. Huang, J.-W. Huang, and W.-C. Liang, "A particle swarm optimization-based maximum power point tracking algorithm for PV systems operating under partially shaded conditions," *IEEE Trans. Energy Convers.*, vol. 27, no. 4, pp. 1027–1035, Dec. 2012.

[4] K. Sundareswaran, S. Peddapati, and S. Palani, "MPPT of PV systems under partial shaded conditions through a colony of flashing fireflies," *IEEE Trans. Energy Convers.*, vol. 29, no. 2, pp. 463–472, Jun. 2014.

[5] R. K. Lenka, A. K. Panda, R. Patel, and J. M. Guerrero, "PV integrated multifunctional off-board EV charger with improved grid power quality," *IEEE Trans. Ind. Appl.*, vol. 58, no. 5, pp. 5520–5532, Sep./Oct. 2022.

[6] G. R. C. Mouli, J. Schijffelen, M. van den Heuvel, M. Kardolus, and P. Bauer, "A 10 kW solar-powered bidirectional EV charger compatible with chademo and COMBO," *IEEE Trans. Power Electron.*, vol. 34, no. 2, pp. 1082–1098, Feb. 2019.

[7] S. A. Singh, G. Carli, N. A. Azeez, and S. S. Williamson, "Modeling, design, control, and implementation of a modified Z-source integrated PV/grid/EV DC charger/inverter," *IEEE Trans. Ind. Electron.*, vol. 65, no. 6, pp. 5213–5220, Jun. 2018.

[8] P. S. Subudhi, S. Padmanaban, F. Blaabjerg, and D. P. Kothari, "Design and implementation of a PV-fed grid-integrated wireless electric vehicle battery charger present in a residential environment," *IEEE J. Emerg. Sel. Topics Ind. Electron.*, vol. 4, no. 1, pp. 78–86, Jan. 2023.

[9] J. Traube et al., "Mitigation of solar irradiance intermittency in photovoltaic power systems with integrated electric-vehicle charging functionality," *IEEE Trans. Power Electron.*, vol. 28, no. 6, pp. 3058–3067, Jun. 2013.

[10] D. Mishra, B. Singh, and B. K. Panigrahi, "Adaptive current control for a bidirectional interleaved EV charger with disturbance rejection," *IEEE Trans. Ind. Appl.*, vol. 57, no. 4, pp. 4080–4090, Jul./Aug. 2021.

[11] R. Kahani, M. Jamil, and M. T. Iqbal, "An improved perturb and observed maximum power point tracking algorithm for photovoltaic power systems," *IEEE J. Modern Power Syst. Clean Energy*, early access, Oct. 28, 2022, doi: 10.35833/MPCE.2022.000245.

[12] M. A. S. Masoum, H. Dehbonei, and E. F. Fuchs, "Theoretical and experimental analyses of photovoltaic systems with voltage and current-based maximum power-point tracking," *IEEE Trans. Energy Convers.*, vol. 17, no. 4, pp. 514–522, Dec. 2002.

[13] B. Revathi, A. Ramesh, S. Sivanandhan, T. B. Isha, V. Prakash, and S. G., "Solar charger for electric vehicles," in *Proc. Int. Conf. Emerg. Trends Innov. Eng. Technol. Res. (ICETIETR)*, 2018, pp. 1–4.

[14] H. K. Singh and N. Kumar, "Solar PV array powered ON board electric vehicle charging with charging current protection scheme," in *Proc. IEEE Int. Conf. Power Electron. Drives Energy Syst. (PEDES)*, 2020, pp. 1–5.
[15] L. Mokgonyana, K. Smith, and S. Galloway, "Reconfigurable low voltage direct current charging networks for plug-in electric vehicles," *IEEE Trans. Smart Grid*, vol. 10, no. 5, pp. 5458–5467, Sep. 2019.
[16] J. S. Oliver, P. W. David, P. K. Balachandran, and L. Mihet-Popa, Analysis of grid-interactive PV-fed BLDC pump using optimized MPPT in DC–DC converters. *Sustainability*, vol. 14, no. 12, p. 7205, 2022.

NISHANT KUMAR (Senior Member, IEEE) received the M.Tech. (with Gold Medal) degree in electrical power systems from the National Institute of Technology Durgapur, India, in 2013, and the Ph.D. degree in power systems from the Department of Electrical Engineering, Indian Institute of Technology (IIT) Delhi, India, in 2019.

He was a Postdoctoral Researcher with the National University of Singapore, Singapore, in 2021. He is currently an Assistant Professor with the Department of Electrical Engineering, IIT Jodhpur, India. He has more than 60 papers in world-renowned journals and ten patents. His research interests include intelligent control of distributed generations and microgrids, cyber security for critical infrastructure, electric vehicle charging infrastructure, and application of soft computing techniques to power system planning, operation, and control.

Dr. Kumar was the recipient of more than 20 national or international awards, such as the IEEE IAS society Best Thesis Award in 2020 and the IEEE (India Section) Best Volunteer Award in 2020.

HARSHIT KUMAR SINGH received the B.Tech. degree in electrical and electronics engineering from the ITS Engineering College, Dr. A.P.J. Abdul Kalam Technical University, India, in 2021. He is currently pursuing the Master of Science by Research [MS(R)] degree with the Department of Electrical Engineering, Indian Institute of Technology Delhi, India. He was the recipient of more than 10 national/international awards, such as "1st Position in 6th International Exhibition and Conference GRIDTECH 2019," "Top 17 in India, in The GoI MHRD–All India Council for Technical Education (AICTE) Incubation Funding 2019," "Top 21 Teams in Himalayan Startup Trek 2019 Pre-Incubation 2019," "1st Position in Sharda University's State-Level Technovation Hackathon 2020," "2nd Position in Dr. Abdul Kalam Technical, Literary and Management Fest 2019," and "1st Position in Kalam Annual Project and Poster Technical Competition (KAPPTeC) 2019."

ROLAND NIWAREEBA (Member, IEEE) received the B.Eng. degree in telecommunication engineering from Kyambogo University, Kampala, Uganda, in 2010, and the M.Sc. degree in microlectronic and communications engineering from Northumbria University, U.K., in 2012 under the Common Wealth Shared Scholarship. In 2015, he joined Kyambogo University as a Member of Academic Staff, where he served as the Head of the Department of Electrical and Electronic Engineering from 2016 to 2019. He has interest in academic and passion for teaching, research, and student mentorship. His research interests are mainly in visible light communication, free-space optical communication, and renewable energy systems. From 2017 to 2020, he served as the Secretary and later the Vice Chair of IEEE Uganda Section and a Branch Counselor of the IEEE Kyambogo University Student Branch.